



# AMSR-E/Aqua Daily L3 12.5 km Brightness Temperature, Sea Ice Concentration, & Snow Depth Polar Grids, Version 4

---

## USER GUIDE

### How to Cite These Data

As a condition of using these data, you must include a citation:

Markus, T., J. C. Comiso, L. Boisvert, and W. N. Meier. 2025. *AMSR-E/Aqua Daily L3 12.5 km Brightness Temperature, Sea Ice Concentration, & Snow Depth Polar Grids, Version 4*. [Indicate subset used]. Boulder, Colorado USA. NASA National Snow and Ice Data Center Distributed Active Archive Center. <https://doi.org/10.5067/J00N1DZZHGW9>. [Date Accessed].

FOR QUESTIONS ABOUT THESE DATA, CONTACT [NSIDC@NSIDC.ORG](mailto:NSIDC@NSIDC.ORG)

FOR CURRENT INFORMATION, VISIT [https://nsidc.org/data/AE\\_S112](https://nsidc.org/data/AE_S112)



National Snow and Ice Data Center

# TABLE OF CONTENTS

1	DATA DESCRIPTION.....	2
1.1	Parameters .....	2
1.2	File Information .....	2
1.2.1	Format .....	2
1.2.2	Data Fields .....	2
1.2.3	Ancillary Data .....	4
1.3	File Naming Convention.....	5
1.4	Spatial Information .....	6
1.4.1	Coverage .....	6
1.4.2	Resolution.....	7
1.4.3	Geolocation .....	7
1.5	Temporal Information.....	9
1.5.1	Coverage .....	9
1.5.2	Resolution.....	9
2	DATA ACQUISITION AND PROCESSING .....	9
2.1	Background.....	9
2.2	Acquisition .....	10
2.3	Processing .....	10
2.3.1	Sea Ice Concentration .....	10
2.3.2	Sea Ice Concentration Difference.....	11
2.3.3	Snow Depth on Sea Ice .....	12
2.4	Quality Assessment .....	12
2.4.1	Automatic QA.....	12
2.4.2	Science QA.....	12
2.5	Error Sources.....	13
2.6	Instrumentation .....	14
3	VERSION HISTORY .....	14
4	SOFTWARE AND TOOLS.....	14
4.1	Geolocation.....	14
4.2	Land Masks.....	14
5	REFERENCES AND RELATED PUBLICATIONS .....	15
6	RELATED DATA SETS .....	16
7	CONTACTS AND ACKNOWLEDGMENTS.....	17
8	DOCUMENT INFORMATION.....	17
8.1	Publication Date.....	17
8.2	Date Last Updated .....	17

# 1 DATA DESCRIPTION

## 1.1 Parameters

---

This data set (AE\_SI12) reports average daily, 12.5 km resolution, horizontally and vertically polarized brightness temperatures ( $T_b$ ) at four frequencies—18.7 GHz, 23.8 GHz, 36.5 GHz and 89.0 GHz. It also reports daily sea ice concentrations derived using the Enhanced NASA Team (NT2) algorithm; daily sea ice concentration differences between the NT2 and the legacy AMSR Basic Bootstrap Algorithm (ABA); and daily snow depths over sea ice. Data are provided on Northern and Southern Hemisphere, polar stereographic grids.

The data are derived from observations acquired by the Advanced Microwave Scanning Radiometer for EOS (AMSR-E).

## 1.2 File Information

---

### 1.2.1 Format

Data are provided in Hierarchical Data Format - Earth Observing System 5 (HDF-EOS5).

### 1.2.2 Data Fields

$T_{bs}$ , sea ice concentrations, sea ice concentration differences, and daily snow depths over ice are written as 2-byte, signed data fields to separate North and South Pole data groups as follows:

HDFEOS/GRIDS/NpPolarGrid12km/Data Fields/

HDFEOS/GRIDS/SpPolarGrid12km/Data Fields/

The NpPolarGrid12km and SpPolarGrid12km data groups also contain latitude and longitude grids, named “lat” and “lon”, respectively, plus the NetCDF dimension scales<sup>1</sup> “XDim” and “YDim”.

#### 1.2.2.1 Naming Convention

Daily average horizontally polarized (H) and vertically polarized (V)  $T_{bs}$ , at each frequency (F), sea ice concentrations, and sea ice concentration differences are reported for ascending orbits (ASC), descending orbits (DSC), and as a daily average (DAY). Five-day snow depths over sea ice are reported as a single value.

---

<sup>1</sup>For more information about NetCDF dimension scales, see [NetCDF-4 Dimensions and HDF5 Dimension Scales](#).

Data fields are named according to the following convention:

**Example**

- SI\_12km\_NH\_18H\_ASC
- SI\_12km\_NH\_ICECON\_ASC
- SI\_12km\_NH\_ICEDIFF\_ASC
- SI\_12km\_NH\_SNOWDEPTH\_5DAY

**Naming Convention**

SI\_12km\_[HEM]\_[PARAM]\_[ORBIT]

The variables above are described in Table 1:

Table 1. Data Field Variable Names and Descriptions

Variable Name	Description
SI_12km	Sea ice, 12.5 km resolution
HEM	NH (N. Hemisphere) or SH (S. Hemisphere)
PARAM	One of: <ul style="list-style-type: none"> <li>• FPOL (frequency and polarization): E.g., 18H = 18.7 GHz, horizontal polarization; 18V = 18.7 GHz, vertical polarization</li> <li>• ICECON: Sea ice concentration (NT2)</li> <li>• ICEDIFF: Sea ice concentration difference (ABA-NT2)</li> <li>• SNOWDEPTH</li> </ul>
ORBIT	One of: <ul style="list-style-type: none"> <li>• ASC (ascending average)</li> <li>• DSC (descending average)</li> <li>• DAY (daily average)</li> <li>• 5DAY (5-day snow depth)</li> </ul>

1.2.2.2 Brightness Temperature ( $T_{bs}$ )

$T_{bs}$  are scaled by a factor of 10 (i.e., have a scale factor = 0.1) when written to the data fields. To recover  $T_{bs}$  in kelvins, multiply the stored value by 0.1. E.g., a stored value of 2673 = 267.3 K. Missing data are denoted by a value of 0.

### 1.2.2.3 Sea Ice Concentration

Sea ice concentrations are reported as percentages, with values ranging from 1 to 100. A value of 0 = open water, 110 = missing, and 120 = land.

### 1.2.2.4 Sea Ice Concentration Difference

Sea ice concentration differences, calculated as  $ICEDIFF = ABA - NT2$ , are provided for users who wish to recover the value of the legacy ABA algorithm (i.e.,  $ABA = ICECON + ICEDIFF$ ). However, this approach is not without its quirks. For example, in pixels flagged as land (120) by both the ABA and NT2 algorithms, differencing these values produces “0,” the value ICECON uses to identify open ocean. Furthermore, because the algorithms utilize different land masks, the same pixel may be flagged as land (120) by one algorithm and open water (0) by the other. As such, ICEDIFF should be used with caution.

### 1.2.2.5 Five-Day Snow Depth

Daily snow depths, computed as the five-day running mean<sup>2</sup>, are reported in centimeters for all Arctic and Antarctic sea ice, excluding regions of perennial Arctic ice. A value of 110 = missing, 120 = land, 130 = open water, 140 = multiyear sea ice, 150 = variability in snow depth, 160 = snow melt.

The CoreMetadata.0 and StructMetadata.0 HDF-EOS global attributes are stored in HDFEOS INFORMATION data group.

## 1.2.3 Ancillary Data

The HDFEOS INFORMATION data group contains a multiyear sea ice mask (“multiyear mask”) and snow melt mask (“variability 5day”). A default mask is used to initialize the multiyear mask on the first day of mission and also to reset the mask on the first processing date in October of each year. The snow melt mask corresponds to the running 5-day snow melt product, and its date must match that of the multiyear mask. The snow melt mask is reset at the same time as the multiyear mask.

The HDFEOS INFORMATION data group also contains the “date” and initialization year” data fields, which specify the processing date (year, month, day) of the masks and the first year in which the masks were set (or reset) to begin processing, respectively. The CoreMetadata.0 and StructMetadata.0 HDF-EOS global attributes are also stored in this data group.

---

<sup>2</sup>Snow depths are not reported for the first four days of each satellite record. These array locations are instead filled with a value of -1.

## 1.3 File Naming Convention

### Example

AMSR\_E\_L3\_Sealce12km\_V16\_20080207.he5

### Naming Convention

AMSR\_E\_L3\_Sealce12km\_[X][##]\_[YYYYMMDD].[EXT]

The following tables describe the variables in the file naming convention:

Table 2. File Name Variables and Descriptions

Variable	Description
X	Product maturity code: P, B, T, or V (See Table 3)
##	File iteration number
YYYYMMDD	Four digit year, two digit month, two digit day
EXT	One of: <ul style="list-style-type: none"> <li>• he5 (HDF-EOS5)</li> <li>• qa (quality assurance information)</li> <li>• ph (product history)</li> <li>• xml (granule-level science metadata)</li> </ul>

Table 3. Product Maturity Codes

Variables	Description
P	Preliminary - refers to non-standard, near-real-time data available from NSIDC. These data are only available for a limited time until the corresponding standard product is delivered to NSIDC.
B	Beta - indicates a developing algorithm with updates anticipated.
T	Transitional - period between beta and validated where the product is past the beta stage, but not quite ready for validation. This is where the algorithm matures and stabilizes.
V	Validated - products are upgraded to Validated once the algorithm is verified by the algorithm team and validated by the validation teams. Validated products have an associated validation stage. Refer to Table 4 for a description of the stages.

Table 4. Validation Stages

Validation Stage	Description
Stage 1	Product accuracy is estimated using a small number of independent measurements obtained from selected locations, time periods, and ground-truth/field program efforts.
Stage 2	Product accuracy is assessed over a widely distributed set of locations and time periods via several ground-truth and validation efforts.
Stage 3	Product accuracy is assessed, and the uncertainties in the product are well-established via independent measurements made in a systematic and statistically robust way that represents global conditions.

## 1.4 Spatial Information

---

### 1.4.1 Coverage

#### North Polar Grid

N: 90.0°    S: 30.98°    E: 180.0°    W: -180.0°

#### South Polar Grid

N: -39.23°    S: -90.0°    E: 180.0°    W: -180.0°

The above coverages are shown in Figure 1 and Figure 2.

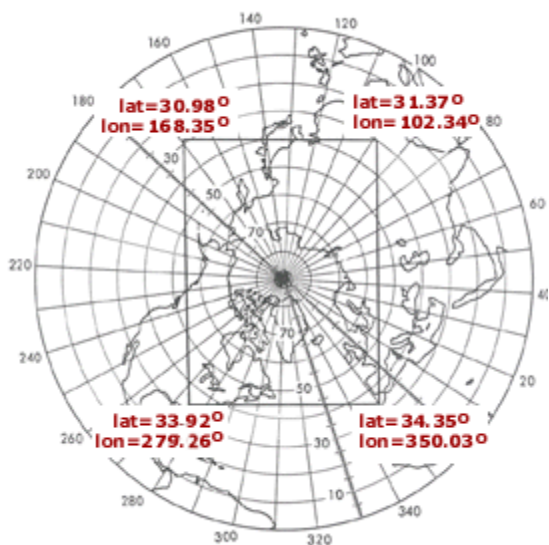


Figure 1. Northern Hemisphere Coverage

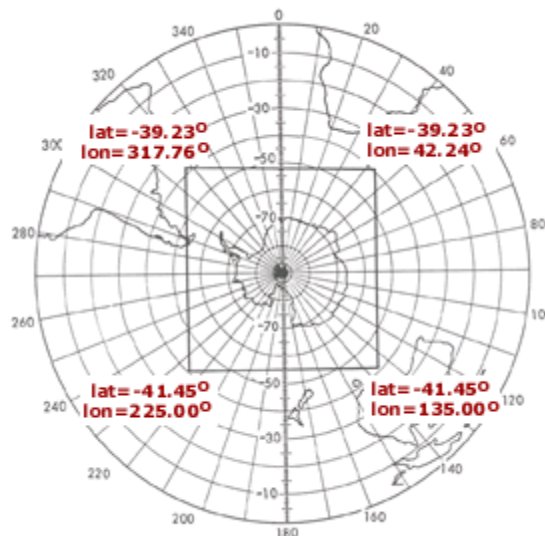


Figure 2. Southern Hemisphere Coverage

## 1.4.2 Resolution

12.5 km

## 1.4.3 Geolocation

The NSIDC polar stereographic grids specify a projection plane tangent to Earth at 70° latitude such that the projection is true at 70° rather than at the poles. This latitude was chosen so that little or no distortion would occur in the marginal ice zone.

The polar stereographic formula for converting between latitude–longitude and X–Y grid coordinates is taken from Snyder (1982). The projection assumes a Hughes ellipsoid with a radius of 6378.273 km (3443.992 nm) and an eccentricity of  $e = 0.081816153$ , or  $e^2 = 0.006693883$ . Note that this value of  $e^2$  is stored to four significant digits (0.006694) in the HDF-EOS5 structural metadata (“HDFEOS INFORMATION/StructMetadata.0”).

The following tables provide information about geolocating this data set:

Table 5. Geolocation Details

Projected coordinate system	NSIDC Sea Ice Polar Stereographic North	NSIDC Sea Ice Polar Stereographic South
Geographic coordinate system	Unspecified datum based upon the Hughes 1980 ellipsoid	Unspecified datum based upon the Hughes 1980 ellipsoid
Longitude of true origin	-45	0

<b>Projected coordinate system</b>	NSIDC Sea Ice Polar Stereographic North	NSIDC Sea Ice Polar Stereographic South
<b>Latitude of true origin</b>	70	-70
<b>Scale factor at longitude of true origin</b>	1	1
<b>Datum</b>	Unspecified, based on Hughes 1980 ellipsoid	Unspecified, based on Hughes 1980 ellipsoid
<b>Ellipsoid/spheroid</b>	Hughes 1980	Hughes 1980
<b>Units</b>	meter	meter
<b>False easting</b>	0	0
<b>False northing</b>	0	0
<b>EPSG code</b>	3411	3412
<b>PROJ4 string</b>	+proj=stere +lat_0=90 +lat_ts=70 +lon_0=-45 +k=1 +x_0=0 +y_0=0 +a=6378273 +b=6356889.449 +units=m +no_defs	+proj=stere +lat_0=-90 +lat_ts=-70 +lon_0=0 +k=1 +x_0=0 +y_0=0 +a=6378273 +b=6356889.449 +units=m +no_defs
<b>Reference</b>	<a href="https://epsg.org/crs_3411/NSIDC-Sea-Ice-Polar-Stereographic-North.html">https://epsg.org/crs_3411/NSIDC-Sea-Ice-Polar-Stereographic-North.html</a>	<a href="https://epsg.org/crs_3412/NSIDC-Sea-Ice-Polar-Stereographic-South.html">https://epsg.org/crs_3412/NSIDC-Sea-Ice-Polar-Stereographic-South.html</a>

Table 6. Grid Details

<b>Hemisphere</b>	<b>North Polar</b>	<b>South Polar</b>
<b>Grid cell size (km)</b>	12.5 × 12.5	12.5 × 12.5
<b>Grid size (rows × columns)</b>	896 × 608	664 × 632
<b>Geolocated lower left point in grid (km)</b>	(-3850, -5350)	(-3950, -3950)
<b>Nominal gridded resolution</b>	12.5 km	12.5 km
<b>Grid rotation</b>	0	0
<b>ulxmap: x-axis coord, center of upper left pixel (XLLCORNER) (km)</b>	-3,843.75	-3,943.75
<b>ulymap: y-axis coord, center of upper left pixel (YLLCORNER) (km)</b>	5,843.75	4,343.75

For additional details about this projection, grid dimensions, and grid coordinates, see [“A Guide to NSIDC's Polar Stereographic Projection.”](#)

## 1.5 Temporal Information

---

### 1.5.1 Coverage

01 June 2002 to 4 October 2011

### 1.5.2 Resolution

Daily

## 2 DATA ACQUISITION AND PROCESSING

### 2.1 Background

---

The NT2 sea ice concentration algorithm represents the most recent version of an approach that began in the 1970s with the “Bootstrap” algorithm. These algorithms—from the original Bootstrap algorithm, the Basic Bootstrap Algorithm (BBA), and the AMSR Bootstrap Algorithm (ABA), through the NASA Team algorithms, NT and NT2—all take advantage of the relatively high contrast in emissivity between open water and sea ice, highlighted by combining different pairs of channel data. Both the Bootstrap and NASA Team algorithms also employ filters to identify and remove spurious sea ice concentration estimates resulting from severe weather.

While the Bootstrap algorithms calculate ice concentrations by interpolating between data clusters in scatterplots of the 19V, 37V, and 37H channels, the NT algorithms compare polarization ratios (PRs) and spectral gradient ratios (GRs). For example, the original NT algorithm used primarily PR(19) and GR(37V19V), computed from the 19V, 19H, and 37V channels as follows:

$$PR(19) = \frac{T_b(19V) - T_b(19H)}{T_b(19V) + T_b(19H)}$$

$$GR(37V19V) = \frac{T_b(37V) - T_b(19V)}{T_b(37V) + T_b(19V)}$$

Similar to the Bootstrap approach, scatterplots of PRs vs GRs tend to cluster around different surface types, such as open ocean, 100% ice coverage, and in the Northern Hemisphere regions of first-year ice and multiyear ice (this distinction is unclear in Antarctica). To determine ice

concentrations, the NT2 algorithm utilizes nine constant coefficients, or “tie points,” each representing a combination of surface type and channel (i.e., 19H, 19V, and 37V).

The enhanced NT2 algorithm (Markus and Cavalieri 2000) additionally incorporates the AMSR-E 89 GHz channels—specifically, PR(89), GR(89V19V), and GR(89H19H)—to resolve ambiguities between pixels with true low ice concentration and pixels with significant surface/weather effects.

While the 89 GHz channels have the added benefit of being relatively insensitive to inhomogeneities in ice surface layer characteristics (e.g., surface temperature variations), they exhibit a higher sensitivity to atmospheric effects. As such, the NT2 also implements a full atmospheric radiative transfer model plus two weather filters, to eliminate the effects of severe weather.

More detailed information is available from the following sources:

- [Descriptions of and differences between the NASA Team and Bootstrap algorithms](#)
- [AMSR-E Algorithm Theoretical Basis Document: Sea Ice Products \[Supplement 2012\]](#)
- [AMSR-E Algorithm Theoretical Basis Document: Sea Ice Products \[Supplement 2007\]](#)

## 2.2 Acquisition

---

This data set is derived from  $T_{bs}$  in the [AMSR-E/Aqua L2A Global Swath Spatially-Resampled Brightness Temperatures \(AE\\_L2A\), Version 4](#) product.

## 2.3 Processing

---

The following sections summarize how the sea ice concentration and snow depth on sea ice calculations are implemented by the NT2 algorithm. For complete details, see “Section 2.2 | Implementation” in “[AMSR-E Algorithm Theoretical Basis Document: Sea Ice Products \[Supplement 2012\]](#)” (AMSR-E Sea Ice Products ATBD, 2012).

### 2.3.1 Sea Ice Concentration

In contrast to algorithms which compute sea ice concentrations from daily, averaged swath  $T_{bs}$ , the NT2 computes sea ice concentrations from individual swath  $T_{bs}$ , and then averages the concentrations to produce daily maps. This approach is critical for the NT2 because the atmospheric influence on  $T_{bs}$  is nonlinear and using averaged  $T_{bs}$  as input would dilute the atmospheric signal.

To determine sea ice concentration, the algorithm first computes  $T_{bs}$  for each AMSR-E frequency/polarization channel corresponding to each sea ice concentration-weather combination.

The response of  $T_{bs}$  to different weather conditions is determined by a forward atmospheric radiative transfer model (Kummerow 1993), that utilizes input data based on Eppler et al. (1992) and includes atmospheric profiles encompassing a range of cloud properties and average atmospheric temperature and humidity profiles for summer and winter conditions.

The algorithm then uses the weather-corrected  $T_{bs}$  to calculate PR and GR ratios and construct look-up tables. These same PR and GR ratios are then computed for the AMSR-E measured  $T_{bs}$  and compared with each of the ratios in the look-up tables to determine observed sea ice concentrations.

This procedure is detailed in “Section 2.2.1 | Calculation of ice concentrations” in the AMSR-E Sea Ice Products ATBD, 2012.

### 2.3.1.1 Land Spillover Correction

Although a land mask is applied to construct the final sea ice concentration maps, land spillover still leads to erroneous ice concentrations along coastlines adjacent to open water. To correct these errors, a five-step, land spillover correction scheme is applied to identify and delete all clearly erroneous ice concentrations. See “Section 2.2.2 | Land Spillover Correction” of the AMSR-E Sea Ice Products ATBD, 2012 for a complete description.

### 2.3.1.2 Weather Filters

Although the NT2 algorithm includes a forward atmospheric radiative transfer to provide weather-corrected sea ice concentrations, severe weather can still result in spurious concentrations over open ocean. As such, the algorithm implements two weather filters based on the spectral gradient ratios GR(37V19V) and GR(22V19V), with threshold values similar to those used by the NT algorithm. These filters are discussed in detail in “Section 2.2.3 | Reduction of Atmospheric Effects” of the AMSR-E Sea Ice Products ATBD, 2012.

## 2.3.2 Sea Ice Concentration Difference

This product also tracks the difference in estimated sea ice concentration between the AMSR-E Bootstrap Algorithm (ABA) and the NT2. This difference is calculated as  $ABA - NT2$ .

For details about the theory behind the ABA and its implementation, the “AMSR-E Bootstrap Sea Ice Algorithm” ATBD is appended to the AMSR-E Sea Ice Products ATBD, 2012 (starting on page 14).

### 2.3.3 Snow Depth on Sea Ice

Snow depth over sea ice is reported as a 5-day running average, based on the current day (i.e., the file name date) and the previous four days. Snow depth on sea ice is calculated using the spectral gradient ratio GR(37V19V) as follows:

$$h_s = a1 + a2 GRV_{ice},$$

where  $h_s$  is the snow depth in meters and  $a1$  and  $a2$  are coefficients derived by a linear regression between in situ snow depth measurements and microwave data.  $GRV_{ice}$  is the GR(37V19V) corrected for the sea ice concentration. In brief, this correction is based on the assumption that scattering increases with increasing snow depth and that the scattering efficiency is greater at 37 GHz than at 19 GHz. For snow-free sea ice, the gradient ratio is close to zero; as snow depth (and grain size) increases, it becomes more and more negative. The correlation between regional in situ and satellite-derived snow depth distributions is 0.81. The upper limit for snow depth retrievals is 50 cm, due to the limited penetration depth of 19 GHz and 37 GHz.

For a more complete description see “Section 3 | Snow Depth on Sea Ice” in the AMSR-E Sea Ice Products ATBD, 2012.

## 2.4 Quality Assessment

---

Each HDF-EOS file contains core metadata with Quality Assessment (QA) metadata flags that are set by the Science Investigator-led Processing System (SIPS) before delivery to NSIDC (this metadata is also available as a separate XML file).

### 2.4.1 Automatic QA

Automatic Weather filters are employed for the Level-3 sea ice products to eliminate spurious sea ice concentrations over open ocean resulting from varying atmospheric emission. The weather filters are based on threshold values for the spectral gradient ratio and thresholds derived from brightness temperature differences. Sea ice products are checked to see if ice concentration values fall within reasonable limits. Diagnostics are based in part on satellite sea ice climatology developed since the Scanning Multichannel Microwave Radiometer (SMMR) era in 1978.

### 2.4.2 Science QA

AMSR-E Level-2A data are subject to science QA in the SIPS environment prior to being processed to higher-level products. Science QA checks for and computes the percentages of missing and out-of-range values for each variable, and if <50% of the data in a file are good, the

file's science QA flag is marked suspect. Science QA also involves reviewing the operational QA files and performing the following additional automated QA procedures (Conway 2002):

- Historical data comparisons
- Detection of errors in geolocation
- Verification of calibration data
- Trends in calibration data
- Detection of large scatter among data points that should be consistent

Once a product passes QA, it is ready to be used for higher-level processing, active science QA, archive, and distribution. Individual files that fail QA are reprocessed before being sent to NSIDC. Files that fail QA are not delivered to NSIDC.

For more information, see the [AMSR-E/Aqua Data Quality and Data Uncertainty](#) document. In addition, users can access [AMSR-E Validation Data](#) that contain details about the accuracy and precision checks conducted on AMSR-E observations.

## 2.5 Error Sources

---

As a result of the spatial averaging when the Level 2A input data are produced, errors in neighboring observations within any single channel will be somewhat correlated (Errors between channels are not correlated in any case). Thus, while the Level 2A data set are well suited for applications that require combining multiple channels of observations, users should be aware that errors in observations within a single channel may not be independent (Ashcroft and Wentz, 2000).

Users should also be aware that the ASC and DSC  $T_b$  averages are not computed as the average of all  $T_b$  observations, but as the average of the ASC and descending DSC averages. This can bias the daily value if, as shown by the following equation, the ASC and DSC averages on a given day were computed from different numbers of observations (i.e.,  $n \neq m$ ):

$$DAY = \frac{\frac{ASC_1 + ASC_2 + \dots + ASC_n}{n} + \frac{DSC_1 + DSC_2 + \dots + DSC_m}{m}}{2}$$

Sources of error in the snow depth on sea ice also include any inherent errors in sea ice concentration; uncertainty in the linear relationship between snow depth and the AMSR-E brightness temperatures; undetected snow wetness; determination of snow grain size and snow density variability; and sensitivity to extreme weather effects.

Finally, although a land mask is applied to the ice concentration maps, land spillover still leads to erroneous ice concentrations along the coastlines adjacent to open water. A land spillover correction scheme is applied on the maps to help mitigate land spillover errors.

## 2.6 Instrumentation

---

Refer to the [AMSR-E Instrument Description document](#).

## 3 VERSION HISTORY

See [AMSR-E Version History](#) for a summary of changes since the start of mission.

## 4 SOFTWARE AND TOOLS

### 4.1 Geolocation

---

Arrays of latitudes and longitudes at grid cell centers of the 12.5 km north and south polar stereographic grids are available in NetCDF format in the [Polar Stereographic Ancillary Grid Information](#) data set. The previous version of these grids (in binary format<sup>3</sup>) can be obtained via an FTP client from:

<ftp://sidacs.colorado.edu/pub/DATASETS/brightness-temperatures/polar-stereo/tools/geo-coord/grid/>

In addition, NSIDC has a Fortran executable (`locate.for`) that allows a user to enter an (i,j) grid coordinate pair and obtain the corresponding latitude and longitude (and vice versa). The `locate.for` executable, its required subroutines, `mapll.for` and `mapxy.for`, plus documentation are available from NSIDC's [GitHub repository](#).

For more information, see “[Does NSIDC have tools to extract and geolocate polar stereographic data? | Geocoordinate tools.](#)”

### 4.2 Land Masks

---

NSIDC provides masks and overlays that can be used, for example, to conceal unwanted northern and southern hemisphere land regions or contaminated coastal ocean pixels incorrectly assigned

---

<sup>3</sup>Latitudes/longitudes are stored as long word integers (4 byte) scaled by 100,000. Each (i,j) array location contains the latitude or longitude value at the center of the corresponding data grid cell.

sea ice concentrations. To determine which masks are available for this data set, see [“Does NSIDC have tools to extract and geolocate polar stereographic data? | Land Masks.”](#)

## 5 REFERENCES AND RELATED PUBLICATIONS

Ashcroft, P. and F. J. Wentz. 2000. *Algorithm Theoretical Basis Document (ATBD): AMSR Level 2A Algorithm*. Revised November 3. Landover, Maryland USA: Goddard Space Flight Center. ([PDF](#))

Cavalieri, D. and J. Comiso. 2000. *Algorithm Theoretical Basis Document for the AMSR-E Sea Ice Algorithm*, Revised December 1. Landover, Maryland USA: Goddard Space Flight Center.

Cavalieri, D. J., K. M. St. Germain, and C.T. Swift. 1995. Reduction of Weather Effects in the Calculation of Sea Ice Concentration with the DMSP SSM/I. *Journal of Glaciology* 41(139): 455-464.

Cavalieri, D. J., P. Gloersen, and W. J. Campbell. 1984. Determination of Sea Ice Parameters with the NIMBUS-7 SMMR. *Journal of Geophysical Research* 89(D4): 5355-5369.

Colbeck, S. C. 1982. An Overview of Seasonal Snow Metamorphism. *Reviews of Geophysics Space Physics* 20:45-61.

Comiso, J., D. Cavalieri, and T. Markus. 2003. Sea Ice Concentration, Ice Temperature, and Snow Depth Using AMSR-E Data. *IEEE Transactions on Geoscience and Remote Sensing* 41(2): 243-252.

Comiso, J. and K. Steffen. 2001. Studies of Antarctic Sea Ice Concentrations from Satellite Data and Their Applications. *Journal of Geophysical Research* 106(C12): 31,361-31,385.

Comiso, J. C., D. J. Cavalieri, C. L. Parkinson, and P. Gloersen. 1997. Passive Microwave Algorithms for Sea Ice Concentration - A Comparison of Two Techniques. *Remote Sensing of the Environment* 60: 357-384.

Comiso, J. C. 1995. *SSM/I Ice Concentrations Using the Bootstrap Algorithm*. NASA RP 1380.

Conway, D. 2002. *Advanced Microwave Scanning Radiometer - EOS Quality Assurance Plan*. Huntsville, AL: Global Hydrology and Climate Center.

Eppler, D. T. and 14 others. 1992. Passive Microwave Signatures of Sea Ice. IN: *Microwave Remote Sensing of Ice. Geophysical Monograph Series* 68: 47-71. Washington, D. C.: American Geophysical Union.

Fraser R. S., N. E. Gaut, E. C. Reifenstein, and H. Sievering. 1975. Interaction Mechanisms Within the Atmosphere Including the Manual of Remote Sensing. *American Society of Photogrammetry* 181-233. Falls Church, VA.

- Gloersen P. and D. J. Cavalieri. 1986. Reduction of Weather Effects in the Calculation of Sea Ice Concentration from Microwave Radiances. *Journal of Geophysical Research* 91(C3): 3913-3919.
- Kelly, R. E., A. T. C. Chang, L. Tsang, and J. L. Foster. 2003. A Prototype AMSR-E Global Snow Area and Snow Depth Algorithm. *IEEE Transactions Geoscience Remote Sensing* 41: 230-242.
- Kummerow, C. 1993. On the Accuracy of the Eddington Approximation for Radiative Transfer in the Microwave Frequencies. *Journal of Geophysical Research* 98: 2757-2765.
- Markus, Thorsten and Donald J. Cavalieri. 2008. [Supplement] AMSR-E Algorithm Theoretical Basis Document: Sea Ice Products. Greenbelt, Maryland USA: Goddard Space Flight Center.
- Markus, T. and D. Cavalieri. 1998. Snow Depth Distribution over Sea Ice in the Southern Ocean from Satellite Passive Microwave Data. IN: *Antarctic Sea Ice: Physical Processes, Interactions, and Variability. Antarctic Research Series* 74: 19-39. Washington, DC: American Geophysical Union.
- Markus, T., D. Cavalieri, and A. Ivanoff. 2011. *Algorithm Theoretical Basis Document for the AMSR-E Sea Ice Algorithm*. Revised December 2011. Landover, MD: Goddard Space Flight Center. ([PDF](#))
- Markus, T. and D. Cavalieri. 2000. An Enhancement of the NASA Team Sea Ice Algorithm. *IEEE Transactions on Geoscience and Remote Sensing* 38: 1387-1398.
- Matzler, C., R. O. Ramseier, and E. Svendsen. 1984. Polarization Effects in Sea-ice Signatures. *IEEE Journal of Oceanic Engineering* 9: 333-338.
- Pearson, F. 1990. *Map projections: Theory and Applications*. Boca Raton, FL: CRC Press.
- Snyder, J. P. 1987. *Map Projections - A Working Manual*. U.S. Geological Survey Professional Paper 1395. U.S. Government Printing Office. Washington, D.C.
- Snyder, J. P. 1982. *Map Projections Used by the U.S. Geological Survey*. U.S. Geological Survey Bulletin 1532.
- Worby, A. P., T. Markus, A. D. Steer, V. I. Lytle, and R. A. Massom. 2008. Evaluation of AMSR-E Snow Depth Product over East Antarctic Sea Ice Using In Situ Measurements and Aerial Photography, *Journal of Geophysical Research* 113(C05): Art. #C05S94.  
doi:10.1029/2007JC004181.

## 6 RELATED DATA SETS

- [Sea Ice Data at NSIDC](#)
- [Sea Ice Trends and Climatologies from SMMR and SSM/I-SSMIS](#)

## 7 CONTACTS AND ACKNOWLEDGMENTS

**Thorsten Markus, Josefino C. Comiso, and Linette Boisvert**

NASA Goddard Space Flight Center

Greenbelt, MD

**Walt N. Meier**

National Snow & Ice Data Center

Boulder, CO

## 8 DOCUMENT INFORMATION

### 8.1 Publication Date

---

July 2025

### 8.2 Date Last Updated

---

July 2025